Controlling chaos with weak periodic signals optimized by a genetic algorithm

C. Y. Soong
Department of Aerospace and System Engineering, Feng Chia University, Seatwen, Taichung, Taiwan 40724, Republic of China

W. T. Huang
Graduate School of Defense Science Studies, Chung Cheng Institute of Technology, National Defense University, Tahsi, Taoyuan, Taiwan 33509, Republic of China

F. P. Lin
Grid Computing Division, National Center of High Performance Computing, Hsinchu, Taiwan 30012, Republic of China

P. Y. Tzeng
Department of Aeronautical Engineering, Chung Cheng Institute of Technology, National Defense University, Tahsi, Taoyuan, Taiwan 33509, Republic of China

(Received 29 October 2003; revised manuscript received 29 March 2004; published 23 July 2004)

In the present study we develop a relatively novel and effective chaos control approach with a multimode periodic disturbance applied as a control signal and perform an in-depth analysis on this nonfeedback chaos control strategy. Different from previous chaos control schemes, the present method is of two characteristic features: (1) the parameters of the controlling signal are optimized by a genetic algorithm (GA) with the largest Lyapunov exponent used as an index of the stability, and (2) the optimization is justified by a fitness function defined with the target Lyapunov exponent and the controlling power. This novel method is then tested on the noted Rössler and Lorenz systems with and without the presence of noise. The results disclosed that, compared to the existing chaos control methods, the present GA-based control needs only significantly reduced signal power and a shorter transient stage to achieve the preset control goal. The switching control ability and the robustness of the proposed method for cases with sudden change in a system parameter and/or with the presence of noise environment are also demonstrated.

DOI: 10.1103/PhysRevE.70.016211 PACS number(s): 05.45.Gg, 87.23.Kg, 02.60.Pn

I. INTRODUCTION

A. Chaos control methods

Chaotic systems are characterized by their extreme sensitivity to the initial conditions; although the chaotic motion may be useful in some cases such as mixing of multicomponent fluid systems and some secure communications. On the other hand, its irregularity and unpredicability are undesirable in most practical applications. For these situations, one may wish to prevent or suppress the occurrence of chaotic behaviors. In the past years, various chaos control methods have been developed. Chaos control approaches can be broadly classified into two categories: feedback and nonfeedback methods. The feedback control chaos methods stabilize one of the unstable periodic orbits (UPOs) embedded in its chaotic attractor by applying small temporal perturbations to an accessible system parameter [1–6]. For some high-speed systems such as chaotic circuits and fast electro-optical systems, there is difficulty in attaining real-time data of the system parameters and variables. In contrast to the feedback control techniques, the nonfeedback methods suppress chaotic motion by changing the system dynamics from a chaotic attractor to a periodic motion [7–18]. Relatively nonfeedback methods have the advantages in speed, flexibility, and no online monitoring and processing required. This class of control approaches is suitable for applications where no real-time or only highly limited measurements of the systems are available.

The nonfeedback methods include introduction of weak periodic parameter perturbation [7–13], constant force or bias [14], weak periodic pulses, open-loop entrainment control [15], and weak noise signals [16]. Comprehensive discussion of a variety of nonfeedback chaos control methods can be found in recent literature, e.g., Refs. [17,18]. For suppression of chaos, to use a weak periodic perturbation signal is simplest and easiest to implement among the existing nonfeedback chaos control methods. In a previous work [7], it has been shown that one of the infinite UPOs embedded in the chaotic attractor can be approached and stabilized by applying a small periodic perturbation to a system parameter or as an external force. Suppressing chaos in a low dimensional system by using a signal of resonant frequency has been confirmed analytically [8] and experimentally [9], and more applications can be found elsewhere, e.g., [10–12].

Recently, Mettin and Kurz [13] proposed an optimization of multiple-mode signals and performed switching control between different target states without the presence of noise. In their method, a cost functional was defined and minimized by an optimization algorithm combining the simulated annealing technique and the downhill simplex method. The functional contains the control signal power as well as a measure of the control performance, i.e., mean recurrence distances. However, the mean recurrence distances may not be defined perfectly, and the performance of optimization has to be improved by a properly selected technique. Furthermore, for systems with a dynamic change in a governing

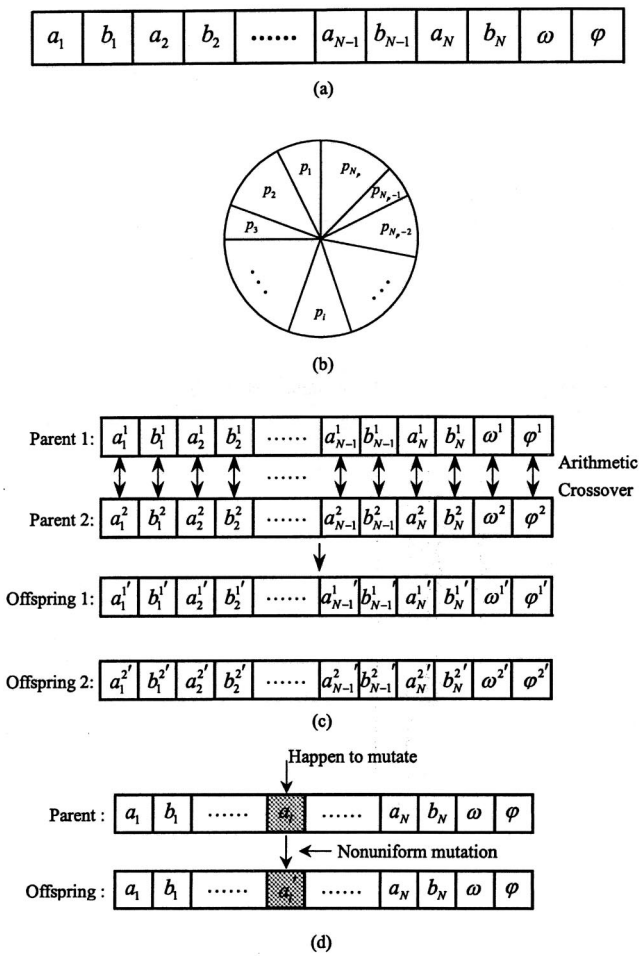

FIG. 1. Illustration of the GA operations used in the present work. (a) Representation of the chromosome; (b) roulette wheel selection; (c) arithmetic crossover operation, and (d) nonuniform mutation operation.

parameter and/or a noisy environment, a more robust control method is needed.

B. Genetic algorithms

Calculus-based search methods usually assume a smooth search space, and most of them use a gradient-following technique. Different from the conventional optimization methods, genetic algorithms (GAs) borrow the concepts and operations from Darwinian evolution [19,20]. Genetic algorithms are inherently a class of global search techniques utilizing the principle of survival of the fittest and have great potential in practical applications. The simulation starts with one set of randomly generated individuals. Each individual in the population representing a solution to the problem is called a *chromosome*. A chromosome is a string of symbols and is usually in the form of a binary bit or floating-point string. The chromosomes evolve through successive iterations and the evolution leads the search toward the area of the best solution. The population in each generation is evaluated by the fitness (or objective) function, which acts as a measure of the adaptability of the solution to the environment. The fitness function guides the searching process without any requirement of derivatives or other auxiliary knowledge. A solution with a higher fitness value is relatively better, although the maximum possible fitness might not be known. The proper choice of the fitness function determines the speed at which the algorithm converges. Then, a new generation can be created by using a *reproduction* operator to select the most fitting individual. To obtain other points in the searching space, after the reproduction, the probabilistic *crossover* and *mutation* operators are applied according to a preset probability for each. Variations are introduced into the new population by means of idealized genetic recombination or crossover operator. The mutation is a random walk process through the string space.

The major characteristics of a GA-based optimization distinct from that of the traditional random search methods are: (a) a GA has a searching direction based on the probabilistic operations; (b) a GA has an evolution mechanism which allows the better strings to generate more offspring; and (c) the average fitness is likely to be improved after some generations.

C. Objective of the present work

In the present study, we attempt to develop an effective and robust approach to suppress chaotic behavior and lead the controlled system to a periodic state even for the systems with a dynamic change in a governing parameter and/or a noisy environment. A genetic algorithm is adopted in the present study for their merits of rapid and efficient global searching ability and effectiveness in optimization problems whose gradient information is not available. The largest Lyapunov exponent is a quantitative measure of chaos and the signal power needed is an index of the performance. Therefore we adopt these two quantities in definition of the fitness function to measure the achievement of the preset control goal and the stability of the stable orbits. The control signal is described by a finite set of real parameters (i.e., Fourier modes) and thus is restricted to a certain control function space. The proposed approach is tested on the noted Rössler [21] and Lorenz [22] systems and the results are compared with previous chaos control methods to demonstrate its superiority.

II. CHAOS CONTROL METHOD WITH GA-OPTIMIZED WEAK PERTURBATION

At first, the evolution dynamics of a system is examined. In power spectra of an uncontrolled system, there appear various modes or UPOs embedded in its chaotic attractor, from which a certain peak is chosen as the target frequency and the searching range of the frequency of the perturbation signal is set around the target mode.

A. Multimode control signals

The general form of the control signals employed in the present analysis is a finite Fourier series up to *N*th order with a zero mean, i.e.,

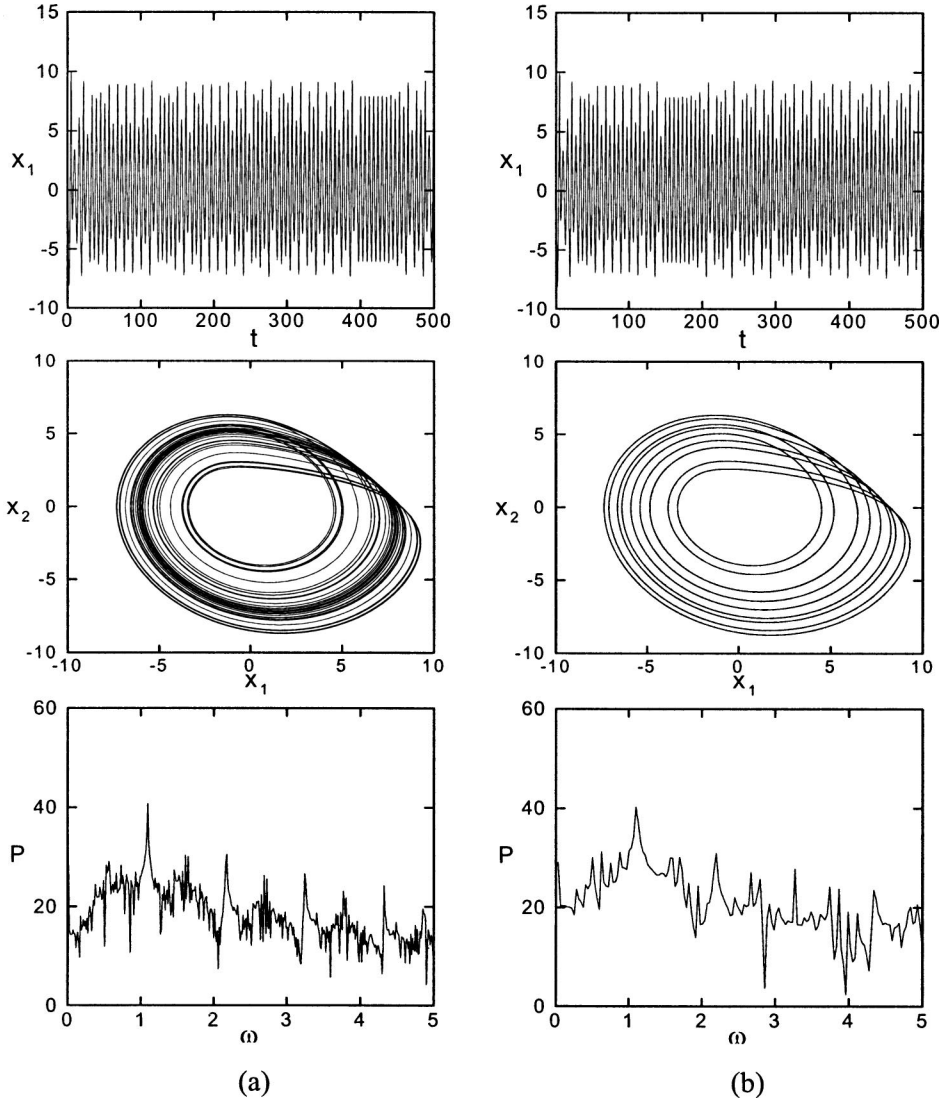

FIG. 2. Time series of x_1, phase trajectory on the x_1-x_2 plane, and power spectrum of the Rössler system with $a=b=0.2$, and $c=4.6$. (a) Uncontrolled chaotic state and (b) period-9 state after control signal $R_{2,0}$ applied at $t=50$.

$$u(t) = \sum_{n=1}^{N} [a_n \cos(n\omega t + \varphi) + b_n \sin(n\omega t + \varphi)], \qquad (1)$$

where a_n and b_n are the amplitudes, $n\omega$ is the frequency of the nth mode, and φ is the phase shift. As that shown in Fig. 1(a), the amplitudes, a_n, b_n, the first-mode frequency ω, and the phase φ play the role of genes to form the chromosome (or individual) and the values of the parameters are to be optimized by evolution of GA. The power of the control signal is expressed in terms of the amplitudes, viz.,

$$P = \frac{1}{2}\sum_{n=1}^{N} (a_n^2 + b_n^2). \qquad (2)$$

Most of the previous studies of chaos control using a weak periodic perturbation set the phase difference as $\varphi=0$. However, the phase φ may play a vital role in suppressing or inducing chaos, especially in nonautonomous systems [23]. In this paper, effects of the phase shift on controlling chaotic autonomous systems are examined.

B. Fitness function

The parameters of the control signals, Eq. (1), are to be optimized by using a genetic algorithm towards the maximum fitness. In the present work, we propose a fitness function, F, defined with consideration of the power of the control signal, P, and the largest Lyapunov exponent, λ_1, calculated from time series of the state variables of the controlled system, viz.,

$$F \equiv \frac{1}{\Delta\lambda^* + P^*}, \qquad (3)$$

where

$$\Delta\lambda^* \equiv |\lambda_1 - \tilde{\lambda}| / \max|\lambda_1 - \tilde{\lambda}|, \; P^* \equiv P/P_m. \qquad (4)$$

In the above expression, the parameter $\Delta\lambda^*$ is the absolute difference between the current value of the largest Lyapunov exponent of the system state λ_1 and the preset target value $\tilde{\lambda}$, normalized by the worst or maximum deviation, $\max|\lambda_1 - \tilde{\lambda}|$, in the current population. The parameter P^* denotes the power of the signal normalized by the maximum power P_m

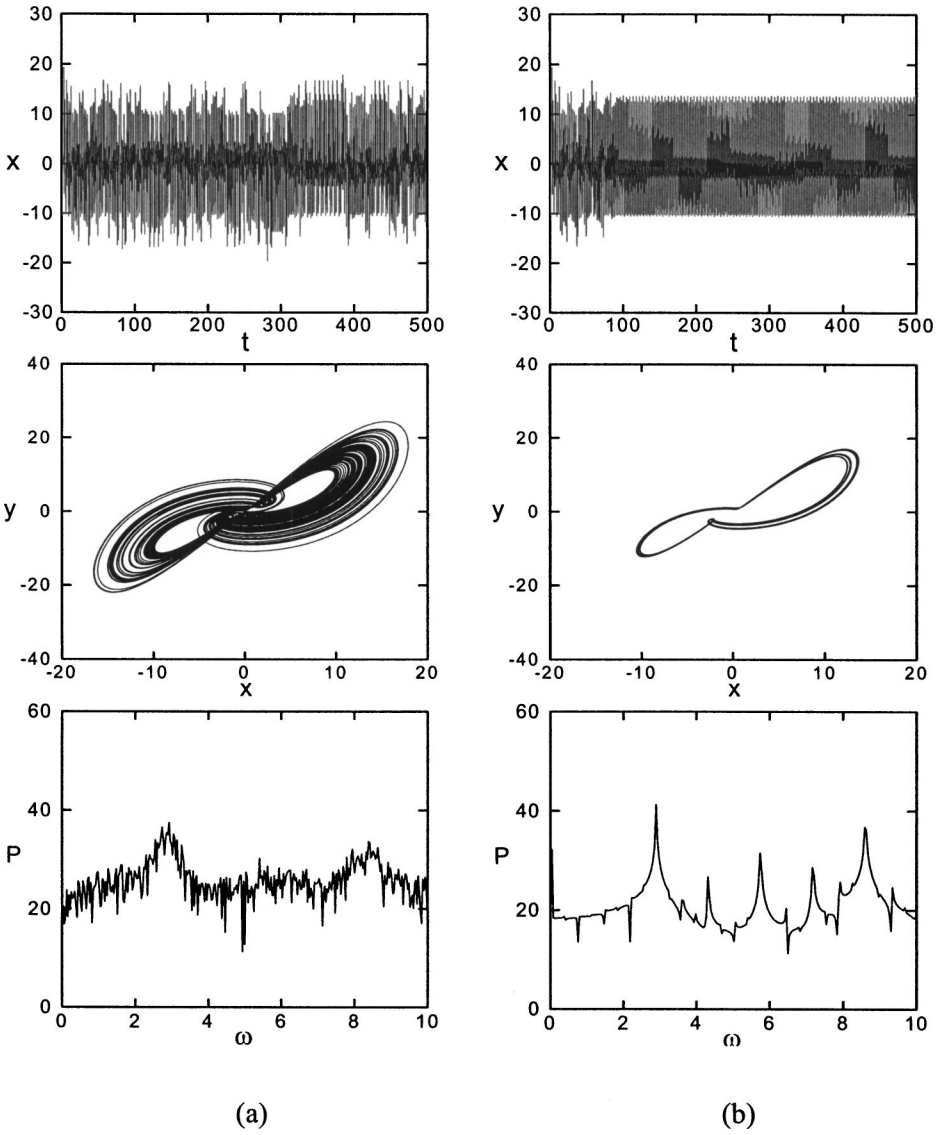

FIG. 3. Time series of x, phase trajectory on the x-y plane, and power spectrum of Lorenz system with Pr=10, b=0.4, and R=80. (a) Uncontrolled chaotic state and (b) period-8 state after a three-mode control signal $L_{3,0}$ ($P=2.014\times10^{-6}$, P-8) applied at t=50.

in the current population. The function F is maximized as $\Delta\lambda^*$ and P^* both approach minimum values. The definition of the fitness function given above can guarantee the stability of the controlled orbits and minimize power required simultaneously. The dynamic behaviors of the chaotic system under control can thus be turned into a periodic motion. The largest Lyapunov exponent can be determined by using the algorithm proposed in [24]. For a periodically perturbed state, the target Lyapunov exponent $\tilde{\lambda}$ has to be set as a nonpositive value and a larger negative value of $\tilde{\lambda}$ implies a more stable target periodic state. To find the minimum power for achieving the control goal is also one of the major concerns.

C. GA process for optimization of control signals

There are many possible variants of the basic genetic algorithm. The steps of the algorithm used in the present work are described as follows with selection, crossover, and mutation operations schematically shown in Fig. 1.

Step 1. Creation of initial population. An initial population of the parent chromosomes is randomly generated with the preset individual length and the population size. As shown in Fig. 1(a), the individual or chromosome is constructed with the parameters of the control signals as genes. Rather than encoded by a binary as the most common representation of a GA, it is more natural to represent the genes directly as real numbers for the parameters in continuous domains. Therefore, the genotype and the corresponding phenotype are of the same type, and better precision and convergence rates can be attained.

Step 2. Evaluation fitness and check stopping criterion. Each member of the current population is evaluated by the fitness function defined in Eq. (3). By using $\lambda_{1,o}$ to denote the largest Lyapunov exponent of the best individual in the current population, stopping criterion can be set as $|\lambda_{1,o}-\tilde{\lambda}|<\varepsilon$. The searching process is terminated if the criterion is satisfied, and the individual of maximum fitness in the current generation is taken as the best solution. Otherwise, the searching procedure continues. The tolerance $\varepsilon=10^{-3}$ is used in the study.

Step 3. Roulette wheel selection. The roulette or propor-

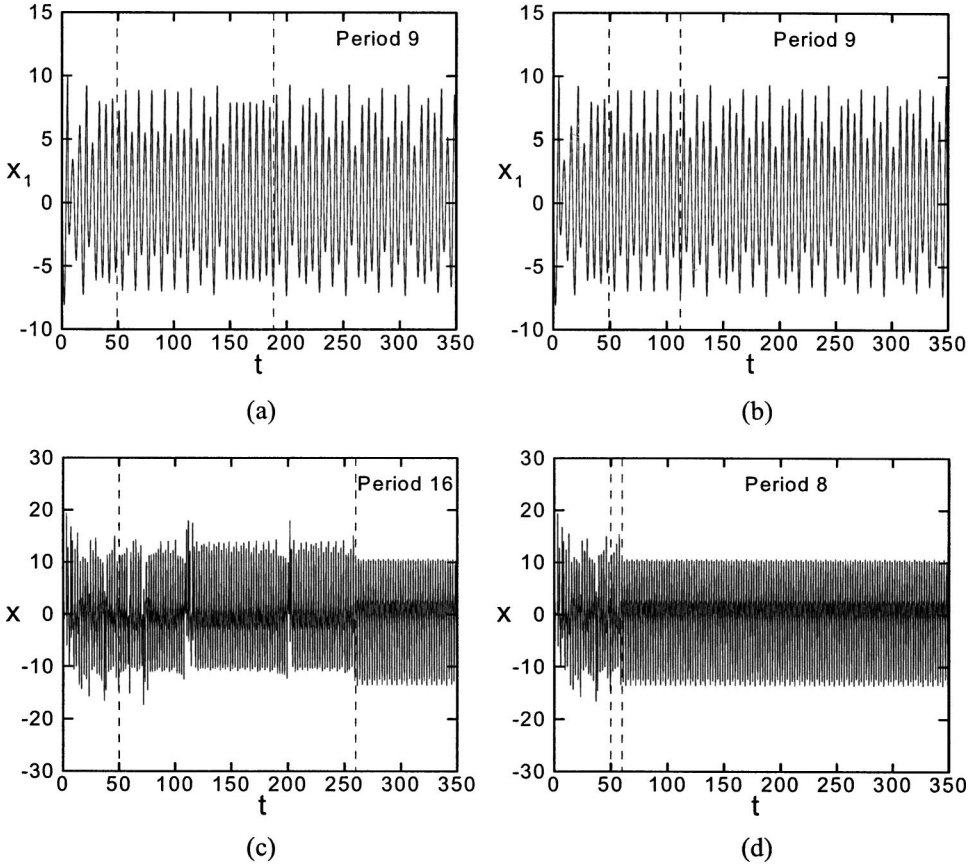

FIG. 4. Time series of chaos and stabilized periodic states by using the different control signals applied at $t=50$, (a) the transient time is 138 for the the Rössler system controlled by a signal without phase modulation ($P=2.15\times10^{-5}$, $a_1=0.006\,423\,30$, $b_1=0.000\,001\,43$, $a_2=0.001\,276\,73$, $b_2=0.000\,428\,26$, $\omega=1.07850773$, $\varphi=0$); (b) the transient time is 61 for the Rössler system controlled by a signal with phase as a parameter, $R_{2,1}$ ($P=2.0\times10^{-5}$); (c) the transient time is 209 for the Lorenz system controlled by a signal without phase modulation ($P=4.0\times10^{-6}$, $a_1=0.000\,182\,69$, $b_1=0.001\,156\,98$, $a_2=0.000\,196\,24$, $b_2=0.002\,568\,11$, $\omega=2.853\,464\,61$, $\varphi=0$); (d) the transient time is 8.6 for the Lorenz system controlled by a signal with phase as a parameter, $L_{2,1}$ ($P=3.82\times10^{-6}$, P-8).

tionate wheel selection schematically shown in Fig. 1(b) is adopted in the algorithm. The selection probability of each individual is evaluated based on its fitness value. For example, with N_p denoting the population size, the selection probability p_i of the ith individual is determined by

$$p_i = F_i \Big/ \sum_{j=1}^{N_p} F_j. \tag{5}$$

Thus a mating pool of N_p individuals is created by selecting from the current population according to the probability of each individual, which is characterized by a randomly selected real number uniformly distributed within the range [0, 1]. If the random value is less than the cumulative probability, the current individual is reproduced to the next generation. The individuals of higher fitness values have more chances to be reproduced. The process is repeated until the entire new population is generated.

Step 4. Probabilistic crossover. The crossover rate p_c given *a priori* determines whether the crossover of two chromosomes occurs. By this genetic operation, a partial exchange of the genetic content between a pair of the members in the population occurs. For the present chromosomes encoded by floating-point, it is appropriate to use an arithmetic crossover defined as two equations of linear combination [20]:

$$\text{new}_1 = \beta\text{old}_1 + (1-\beta)\text{old}_2, \tag{6a}$$

$$\text{new}_2 = (1-\beta)\text{old}_1 + \beta\text{old}_2, \tag{6b}$$

where new_1 and new_2 are the resultant offspring of old_1 and old_2 after the crossover operation. The parameter β can be set as a constant between 0 and 1 (uniform arithmetical crossover) or varies with the number of generations (nonuniform arithmetical crossover).

Step 5. Probabilistic mutation. Mutation occurs to each gene of the chromosomes with a probability, p_m, which is usually small. With the coding representation of real numbers, the mutation will randomly change the value of the chromosome within the range of defined variable space. The nonuniform mutation adopted in the present algorithm is described as follows [20].

Denoting $C^g=(c_1,\ldots,c_k)$ for a chromosome and the element $c_i\in[l_i,u_i]$ in gth generation is supposed to be selected to mutate. The result is a vector $C^{g+1}=(c_1,\ldots,c_i',\ldots,c_k)$ with $i\in\{1,\ldots,k\}$, and

$$c_i' = \begin{cases} c_i + \Delta(g, u_i - c_i) & \text{if } \gamma = 0 \\ c_i + \Delta(g, c_i - l_i) & \text{if } \gamma = 1, \end{cases} \tag{7}$$

where γ is a randomly generated two-valued (0 or 1) index used to determine which one of the two expressions is employed for the evaluation of c_i'. The function $\Delta(g,s)$ is defined as

$$\Delta(g,s) = s[1 - r^{(1 - g/g_{\max})^{b^*}}], \tag{8}$$

in which r is a random number in the interval [0, 1], $g_{\max}$ is the given maximum number of generations, and the user-specified parameter b^* determines the degree of dependence on the number of iterations. The function $\Delta(g,s)$ gives a value in the range $[0,s]$ such that the probability of mutation diminished as $g \to g_m$. This property renders this operator to search the space uniformly as g is small initially but very locally at later stages, and thus increases the probability of generating a new number closer to its successor than a random choice.

Step 6. Application of elitism strategy. New offspring are generated and each member of the offspring is then evaluated by the defined fitness function. To improve the convergence rate, an elitism strategy, i.e., 50% of individuals with high fitness values, is selected from the pool of the parents as well as the offspring to update the resultant population and then go back to step 2.

D. Numerical details

The simulation procedures are coded in C-language. The fourth-order Runge-Kutta integration method is used to solve the evolution equations with given initial conditions. In the present simulation, the population size $N_p = 200$, the crossover rate $p_c = 0.7$, the constant $\beta = 0.95$, and the mutation parameters $p_m = 0.4$ and $b^* = 0.1$ are adopted. Usually, time-step (Δt) of the order 10^{-1} or 10^{-2} are used for simulation of the Rössler system and 10^{-2} for the Lorenz system [25–28]. In the present study, smaller time-step sizes of $\Delta t = 5 \times 10^{-2}$ and 5×10^{-3} are employed for the Rössler system and Lorenz system, respectively.

Lyapunov exponents are calculated by the algorithm proposed by Wolf *et al.* [24]. With time-step in a wide range, $\Delta t = 5 \times 10^{-3} - 10^{-1}$ and the time series length of 400 time units ($t = 100 - 500$), the value of λ_1 span over the range of 0.1238–0.1275 for the Rössler system, and 2.1507–2.1644 for Lorenz system with $\Delta t = 10^{-4} - 10^{-2}$. With $\Delta t = 5 \times 10^{-3}$ and the time series length of 100 ($t = 400 - 500$) to 400 time units ($t = 100 - 500$), the calculated λ_1 lies in the range of 2.1634–2.1695. In the form of (mean) $\pm$ (sample standard deviation), the above data for the Rössler system can be expressed as 0.12545 ± 0.00153 and that for the Lorenz system as 2.16206 ± 0.00730. The results demonstrate that, at least in the ranges we considered, the calculated λ_1 is not very sensitive to the time-step size and the length of the time series.

In the present study, the searching interval for frequency ω is selected around a resonant frequency, the interval $[-2\pi, 2\pi]$ is for searching phase φ, and the interval [0, 0.01] is usually assigned for optimization of the amplitudes a_i and b_i. While an extended interval can be employed as a signal of higher power is desired.

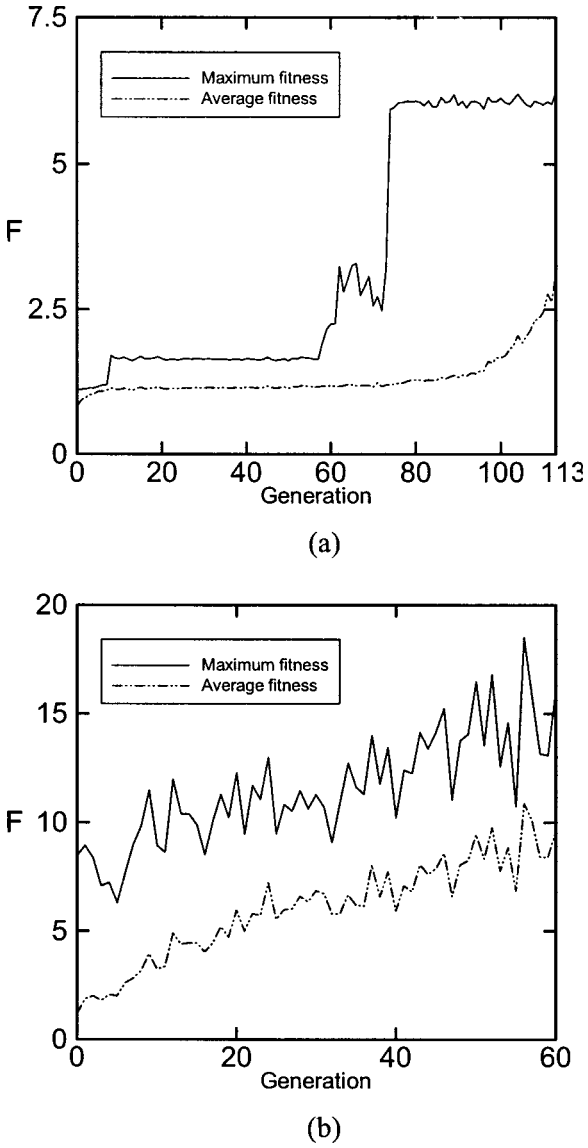

FIG. 5. Variations of maximum and averaged fitness values during the evolution of the population for optimization of control signals. (a) Rössler system with optimized signals $R_{2,0}$ and (b) Lorenz system with optimized signal $L_{3,0}$.

III. RESULTS AND DISCUSSION

In this section, we show a series of numerical simulations to demonstrate the effectiveness and robustness of the proposed method under various conditions. Two noted nonlinear systems with a perturbation signal $u(t)$ involved are employed as the test models. The first one is the Rössler system:

$$\dot{x}_1 = -x_2 - x_3 + u(t),$$

$$\dot{x}_2 = x_1 + a x_2, \tag{9}$$

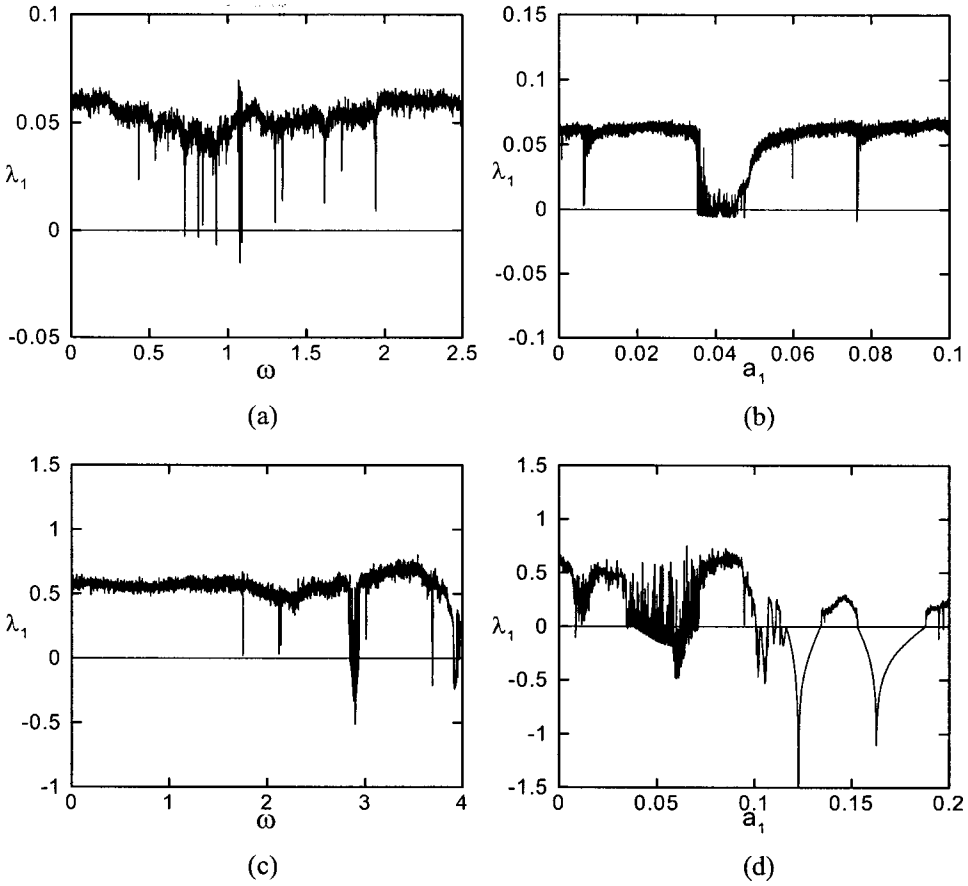

FIG. 6. Variations of the largest Lyapunov exponent vs the perturbation frequency and amplitude, (a) Rössler system with $a_1=0.1$, (b) Rössler system with $\omega=1.0789$, (c) Lorenz system with $a_1=0.05$, and (d) Lorenz system with $\omega=2.86$.

$$\dot{x}_3 = x_1 x_3 - c x_3 + b,$$

in which a, b, and c are system parameters, and the perturbation $u(t)$ acts as an external control force applied on the first component of the vector $\mathbf{x}=(x_1,x_2,x_3)$. The second model is the Lorenz system:

$$\dot{x} = \Pr(y - x),$$

$$\dot{y} = -xz + R[1 + u(t)]x - y, \tag{10}$$

$$\dot{z} = xy - bz.$$

where the three system parameters are Pr standing for Prandtl number, R for normalized Rayleigh number, and b for geometry of the system. Different from the Rössler system, the Lorenz system is used to study the effects of the perturbation in a system parameter, i.e., R in this model. The present GA-based method with control signals of one mode ($N=1$) up to five modes ($N=5$) is studied and the results without phase shift ($\varphi=0$) are compared with the results of the non-GA-based control performed by Mettin and Kurz [13].

To designate various control signals with different modes and conditions, the notations $R_{N,M}$ and $L_{N,M}$ are, respectively, used for the Rössler and Lorenz systems, in which the subscript N is the number of mode. The subscript M is an index for designation of various signals with the same mode N, and the special one of $M=0$ denotes the signals with zero phase shift $\varphi=0$, which was considered in the previous studies, e.g., [10,13].

A. Fundamental features of the control strategy

To verify the effectiveness of the present GA-based method, results are compared with that by the previous chaos control methods, e.g., Ref. [13]. First, the weak periodic perturbation control of the Rössler system is performed. The system parameters are set to be $a=b=0.2$ and $c=4.6$, which correspond to a chaotic attractor. The power spectrum of the uncontrolled Rössler system is shown in Fig. 2(a). It is observed that the strongest energy-contained mode is that of the frequency $\omega=1.099$. To compare with the results of Mettin and Kurz, at first, the same conditions of $\varphi=0$ and $b_1=0$ of the control signal and the searching range of frequency interval $\omega \in [0.520, 0.562]$ are considered for comparison. Then the optimization of control signal with perturbation frequency in the interval $\omega \in [1.0, 1.1]$ is also performed.

Simulations are performed with initial condition $\mathbf{x}(0)=(5.0,5.0,5.0)$ and time step $\Delta t=5\times10^{-2}$. The control signal is applied to the system at the time instant $t=50$. The control target is set to be a state with the largest Lyapunov exponent $\tilde{\lambda}=0$. The optimum Fourier coefficients (amplitudes), frequencies, and powers for the control signals under consideration are shown in Table I. It is revealed that the necessary powers of control signal obtained by the present method are significantly lower, e.g., the controlling power

TABLE I. Comparison of amplitudes, frequencies, and powers of the optimized periodic signals for chaos control of the Rössler system by the present and Mettin-Kurz [13] methods. (NA denotes not available.)

	Present				Mettin-Kurz
	$\omega \in [1.0, 1.1]$		$\omega \in [0.520, 0.562]$		$\omega \in [0.520, 0.562]$
Signal	Amplitudes and frequency	Power (period-k)	Amplitudes and frequency	Power (period-k)	Power (period-k)
$R_{1,0}$	$a_1 = 0.006\,404\,60$ $\omega = 1.078\,861\,72$	$P = 2.05 \times 10^{-5}$ (P-9)	$a_1 = 0.148\,293\,15$ $\omega = 0.538\,191\,37$	$P = 1.10 \times 10^{-2}$ (P-8)	$P = 2.23 \times 10^{-2}$ (NA)
$R_{2,0}$	$a_1 = 0.006\,235\,30$ $a_2 = 0.001\,012\,61$ $b_2 = 0.000\,007\,84$ $\omega = 1.078\,821\,98$	$P = 2.00 \times 10^{-5}$ (P-9)	$a_1 = 0.000\,000\,17$ $a_2 = 0.006\,378\,30$ $b_2 = 0.000\,057\,46$ $\omega = 0.539\,315\,31$	$P = 2.03 \times 10^{-5}$ (P-9)	$P = 9.95 \times 10^{-3}$ (NA)
$R_{3,0}$	$a_1 = 0.006\,285\,42$ $a_2 = 0.001\,023\,36$ $b_2 = 0.000\,005\,95$ $a_3 = 0.000\,061\,31$ $b_3 = 0.000\,100\,27$ $\omega = 1.078\,828\,09$	$P = 2.03 \times 10^{-5}$ (P-9)	$a_1 = 0.000\,009\,61$ $a_2 = 0.006\,412\,48$ $b_2 = 0.000\,016\,51$ $a_3 = 0.000\,059\,14$ $b_3 = 0.000\,121\,73$ $\omega = 0.539\,438\,71$	$P = 2.06 \times 10^{-5}$ (P-9)	$P = 5.42 \times 10^{-3}$ (NA)
$R_{5,0}$	$a_1 = 0.006\,518\,76$ $a_2 = 0.001\,386\,62$ $b_2 = 0.000\,831\,98$ $a_3 = 0.000\,000\,64$ $b_3 = 0.000\,002\,92$ $a_4 = 0.000\,105\,94$ $b_4 = 0.000\,048\,45$ $a_5 = 0.000\,035\,74$ $b_5 = 0.000\,012\,22$ $\omega = 1.078\,392\,52$	$P = 2.26 \times 10^{-5}$ (P-9)	$a_1 = 0.000\,015\,64$ $a_2 = 0.006\,375\,42$ $b_2 = 0.000\,004\,67$ $a_3 = 0.000\,001\,74$ $b_3 = 0.000\,002\,01$ $a_4 = 0.000\,835\,67$ $b_4 = 0.000\,001\,45$ $a_5 = 0.000\,009\,34$ $b_5 = 0.000\,002\,06$ $\omega = 0.539\,284\,93$	$P = 2.07 \times 10^{-5}$ (P-9)	$P = 2.04 \times 10^{-3}$ (P-3)

found by the GA-based method with the signal $R_{2,0}$ ($\omega \in [1.0, 1.1]$) is even smaller than 1% of the power of signal $R_{5,0}$ proposed in [13]. Control effectiveness can be demonstrated from the periodic state of period-9 (or simply denoted by P-9) in Fig. 2(b), which is turned from the chaotic state of Fig. 2(a) after the optimized signal $R_{2,0}$ is applied.

It is also shown that the two-mode signal ($N=2$) has remarkably lower power as compared with the single-mode. However, further increase of the number of the modes has no significant advantage in reduction of the power. For the present high effective GA-based method of global search ability, the degrees of freedom for $N=2$ or 3 are sufficient. Adding more modes could result in a minor change, e.g., 10^{-5} or less, in power. Therefore, even for $N=5$, the power of the optimum signal cannot be further reduced but remains as the same order. However, searching for a signal of mode number $N=2$ or 3 needs considerably less computational time in GA optimization, e.g., time for reaching at optimization of a signal $R_{2,0}$ ($N=2$) is only 6.9% of the time needed for $R_{5,0}$ ($N=5$) for the Rössler system.

In the present GA optimization, searching procedures are initiated with randomly selected individuals as the first generation. It is found that the optimized signals generated by using different sets of random populations have the powers of the same order. Nevertheless, employing an optimized n-mode signal as a basic form with an additional mode added to build the $(n+1)$-mode signal, the time taken for optimization of this $(n+1)$-mode signal can be dramatically shortened. For example, to reach optimization of a 4-mode signal with an optimized 3-mode signal as a base takes only about 10% of the time for the searching with randomly selected individuals. However, it has no noticeable advantage in reduction of the signal power needed for control. As an optimized signal is applied to control a chaotic system, using different initial states of the system influences the length of the transient stage, but it cannot change the period number of the final state.

As to the chaotic behavior of the Lorenz system, a typical case at Pr=10, $b=0.4$, and $R=80$ is shown in Fig. 3(a). From the power spectrum of the uncontrolled state, a high energy-contained mode at the frequency appearing around $\omega_0 = 2.84$, the simulation was carried out with the frequency searching interval, $\omega \in [2.7, 3.1]$, the time period $t \in [0, 500]$, time step $\Delta t = 5 \times 10^{-3}$, and the initial condition $(x_0, y_0, z_0) = (0.1, 0.1, 0.1)$. The optimized signals of various modes determined by the present approach are shown in

TABLE II. Comparison of the optimized periodic signals for chaos control of the Lorenz system determined by the present method and Lui-Leite's method [10]. (NA denotes not available.)

	Present		Lui-Leite
Signal	Amplitudes and frequency	Power (period-k)	Power (period-k)
$L_{1,0}$	$a_1=0.008\,064\,77$ $\omega=2.865\,443\,64$	$P=3.252\times10^{-5}$ (P-3)	$P=3.125\times10^{-4}$ (P-1)
$L'_{1,0}$	$a_1=0.012\,486\,36$ $\omega=2.869\,580\,86$	$P=7.8\times10^{-5}$ (P-1)	
$L_{2,0}$	$a_1=0.000\,034\,29$ $a_2=0.000\,575\,57$ $b_2=0.002\,713\,77$ $\omega=2.859\,728\,37$	$P=3.849\times10^{-6}$ (P-4)	NA
$L_{3,0}$	$a_1=0.000\,075\,78$ $a_2=0.001\,562\,58$ $b_2=0.000\,991\,16$ $a_3=0.000\,770\,39$ $b_3=0.000\,074\,24$ $\omega=2.854\,976\,44$	$P=2.014\times10^{-6}$ (P-8)	NA
$L_{5,0}$	$a_1=0.000\,576\,48$ $a_2=0.000\,052\,68$ $b_2=0.002\,922\,41$ $a_3=0.000\,343\,98$ $b_3=0.000\,404\,44$ $a_4=0.000\,084\,53$ $b_4=0.000\,482\,34$ $a_5=0.000\,000\,23$ $b_5=0.000\,420\,19$ $\omega=2.841\,934\,96$	$P=4.787\times10^{-6}$ (P-8)	NA

Table II. The comparison shows that the power of the signals $L_{1,0}$ and $L_{3,0}$ found by the present GA-based optimization are only 10.4% and 0.64%, respectively, of the Lui-Leite's result [10]. Besides, it also shows that increasing the number of Fourier modes does not necessarily reduce the control power. Figure 3(b) reveals that a periodic state of P-8 can be achieved by the present chaos control with the optimized three-mode signal, $L_{3,0}$. With a larger searching range of the amplitudes, we found a one-mode signal $L'_{1,0}$ (in Table II) of a higher power $P=7.8\times10^{-5}$, which can lead the chaotic system to an orbit of P-1. The power of $L'_{1,0}$ is only 25% of that found by Lui and Leite [10].

Figures 4(a) and 4(b), respectively, show the chaos control results of the Rössler system with optimized 2-mode signals without and with phase modulation applied at $t=50$. It reveals that the signal $R_{2,1}$ with φ as one of the signal parameters considerably reduces the transient time period from 138 to 61 time units. The results in Figs. 4(c) and 4(d) are those of the Lorenz system controlled by optimized 2-mode signals without and with phase modulation, respectively. Similarly, the transient time has been minimized from

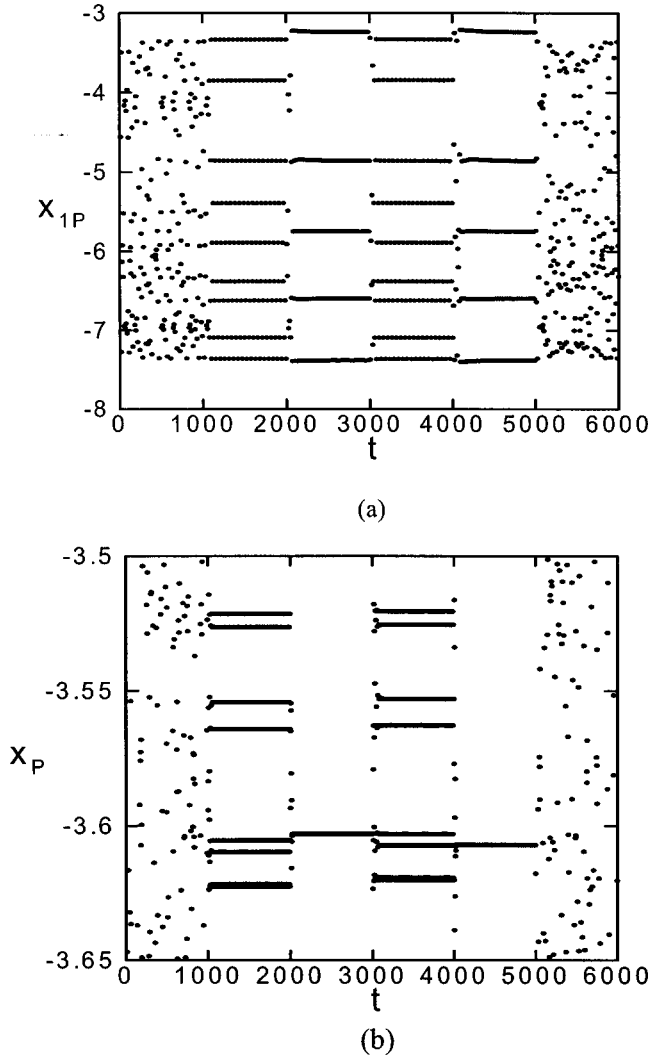

FIG. 7. (a) Switching control of the Rössler system. Control is activated in the time period $t=1000$ to $t=5000$ and switched between $R_{2,1}$ ($P=2.0\times10^{-5}$, P-9) and $R_{2,2}$ ($P=6.41\times10^{-4}$, P-5) every 1000 time units. The phase shifts at various stages are $t=1000$: $\varphi=0.680\,205\,08$; $t=2000$: $\varphi=2.100\,468\,85$; $t=3000$: $\varphi=-5.890\,236\,16$; $t=4000$: $\varphi=-3.088\,813\,90$; the Poincaré section is $x_2=0$; (b) Switching control of the Lorenz system. The signal is switched between $L_{2,1}$ ($P=3.82\times10^{-6}$, P-8) and $L_{2,4}$ ($P=2.63\times10^{-5}$, P-1). The phase shifts at various stages are $t=1000$: $\varphi=-6.249\,884\,43$; $t=2000$: $\varphi=3.274\,711\,35$; $t=3000$: $\varphi=5.807\,548\,18$; $t=4000$; $\varphi=4.212\,247\,43$. The Poincaré section is $y=-5$.

209 to 8.6. It is revealed that, for autonomous systems, the consideration of phase modulation has little benefit to the reduction in signal power but may considerably shorten the transient time during the control.

Figure 5 shows the maximum and averaged fitness values during the evolution of the population for the optimization of the signals $R_{2,0}$ and $L_{3,0}$. Although fluctuations appear, both the maximum and average values of the fitness function present an ascending trend during evolution. It demonstrates that the present method effectively leads the evolution procedure towards the solution of a high fitness.

TABLE III. The amplitudes, frequencies, phases, and powers of various two-mode periodic signals for chaos control of the Rössler and Lorenz systems.

Signal	Amplitudes, frequency, and phase	Power (period-k)	Signal	Amplitudes, frequency, and phase	Power (period-k)
$R_{2,1}$	$a_1=0.004\,805\,86$ $b_1=0.003\,932\,12$ $a_2=0.001\,094\,59$ $b_2=0.000\,515\,84$ $\omega=1.078\,652\,82$ $\varphi=-5.234\,870\,41$	$P=2.0\times10^{-5}$ (P-9)	$L_{2,1}$	$a_1=0.000\,900\,56$ $b_1=0.000\,680\,13$ $a_2=0.002\,121\,33$ $b_2=0.001\,363\,36$ $\omega=2.855\,124\,93$ $\varphi=6.025\,226\,12$	$P=3.82\times10^{-6}$ (P-8)
$R_{2,2}$	$a_1=0.024\,739\,64$ $b_1=0.025\,871\,47$ $a_2=0.000\,368\,35$ $b_2=0.000\,365\,72$ $\omega=1.078\,039\,18$ $\varphi=1.688\,084\,58$	$P=6.41\times10^{-4}$ (P-5)	$L_{2,2}$	$a_1=0.000\,043\,65$ $b_1=0.000\,304\,84$ $a_2=0.003\,120\,92$ $b_2=0.001\,598\,80$ $\omega=2.873\,925\,99$ $\varphi=4.336\,693\,31$	$P=6.20\times10^{-6}$ (P-2)
$R_{2,3}$	$a_1=0.034\,076\,75$ $b_1=0.012\,536\,76$ $a_2=0.000\,497\,81$ $b_2=0.000\,593\,01$ $\omega=1.078\,179\,37$ $\varphi=-3.478\,568\,18$	$P=6.60\times10^{-4}$ (P-5)	$L_{2,3}$	$a_1=0.003\,695\,43$ $b_1=0.000\,503\,93$ $a_2=0.004\,496\,72$ $b_2=0.000\,271\,69$ $\omega=2.847\,096\,83$ $\varphi=-1.890\,718\,84$	$P=1.71\times10^{-5}$ (P-1)
$R_{2,4}$	$a_1=0.171\,806\,30$ $b_1=0.110\,167\,62$ $a_2=0.001\,065\,55$ $b_2=0.005\,500\,15$ $\omega=1.067\,792\,45$ $\varphi=-4.838\,595\,65$	$P=2.08\times10^{-2}$ (P-3)	$L_{2,4}$	$a_1=0.000\,184\,50$ $b_1=0.003\,561\,62$ $a_2=0.006\,306\,10$ $b_2=0.000\,116\,58$ $\omega=2.841\,725\,61$ $\varphi=3.274\,711\,35$	$P=2.63\times10^{-5}$ (P-1)

To examine the effects of the perturbation frequency and amplitudes on the stability characteristics of the controlled system, Fig. 6(a) presents the variation of the largest Lyapunov exponent, λ_1, with the change in the perturbation frequency, ω, at the fixed amplitude $a_1=0.1$; while variations of the largest Lyapunov exponent with the perturbation amplitude a_1 at the fixed frequency $\omega=1.0789$ are shown in Fig. 6(b). The similar characteristics of the Lorenz system are shown in Fig. 6(c) for the variation of λ_1 with the perturbation at $a_1=0.05$ and Fig. 6(d) for that at the fixed frequency, $\omega=2.86$. It is observed that several very narrow periodic windows emerge between the chaotic regions. The deeper valleys appear as the frequency of the control signal approaching the resonant frequency. Several periodic windows emerge at smaller amplitudes. It confirms that weak resonant perturbation signals can be employed to suppress chaos. The amplitude or power and resonant frequency are significant parameters for suppressing chaos.

To bring the system to a state of specified period number (period-k), we need a parameter acting as a quantitative index to characterize the value of k. Unfortunately, to the best of our knowledge, there is still no such kind of target index in the existing chaos control methods. The initial condition has no obvious influence on the power of the optimized signal, it cannot alter the period number of the orbit. Nevertheless, the period number k of the controlled orbit depends on the power of the control signal. For example, with $\tilde{\lambda}=-0.01$, frequency searching range $\omega\in[2.7,3.1]$, and the amplitude searching ranges of [0, 0.01] and [0, 0.1], respectively, we can find a two-mode signal of $P=3.83\times10^{-6}$ for period-8 and a stronger one of $P=6.08\times10^{-4}$ for period-1.

B. Switching control between different states

Figure 7(a) is a typical example of switching control on the Rössler system. The switching signals include the previous signal $R_{2,1}$ (P-9) and another two-mode signal of higher power, $R_{2,2}$ (P-5). The amplitudes, frequencies, phases, and powers of these signals are presented in Table III. The system is initially chaotic until the signal $R_{2,1}$ applied at the time instant $t=1000$. The system behavior is a periodic state (P-9). At $t=2000$, the control signal is replaced by $R_{2,2}$ and a new periodic state of P-5 appears. One more cycle of switching between P-5 and P-9 is subsequently carried out every 1000 time units. Finally, at $t=5000$, the control signal is totally removed and the system returns to the chaotic state. This switching process of the sequence: CA (chaotic attractor) $\rightarrow$P-9$\rightarrow$P-5$\rightarrow$P-9$\rightarrow$P-5$\rightarrow$CA is shown in Fig. 7(a) with

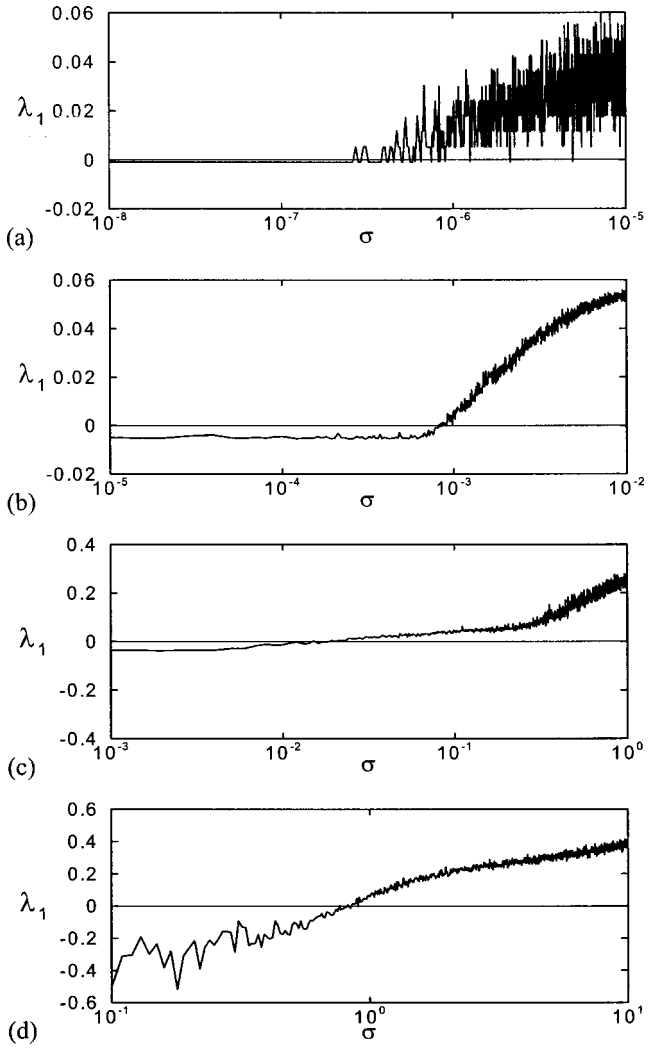

FIG. 8. Influence of Gaussian noise level on the controlled Rössler and Lorenz systems: the largest Lyapunov exponent λ_1 vs the noise level σ with applications of control signals, (a) threshold noise level $\sigma_{\text{th}}=2.7\times10^{-7}$ for $R_{2,1}$ (P-9), (b) threshold noise level $\sigma_{\text{th}}=8.2\times10^{-4}$ for $R_{2,2}$ (P-5), (c) threshold noise level threshold $\sigma_{\text{th}}=1.5\times10^{-2}$ for $L_{2,1}$ (P-8), and (d) threshold noise level $\sigma_{\text{th}}=7.6\times10^{-1}$ for $L_{2,4}$ (P-1).

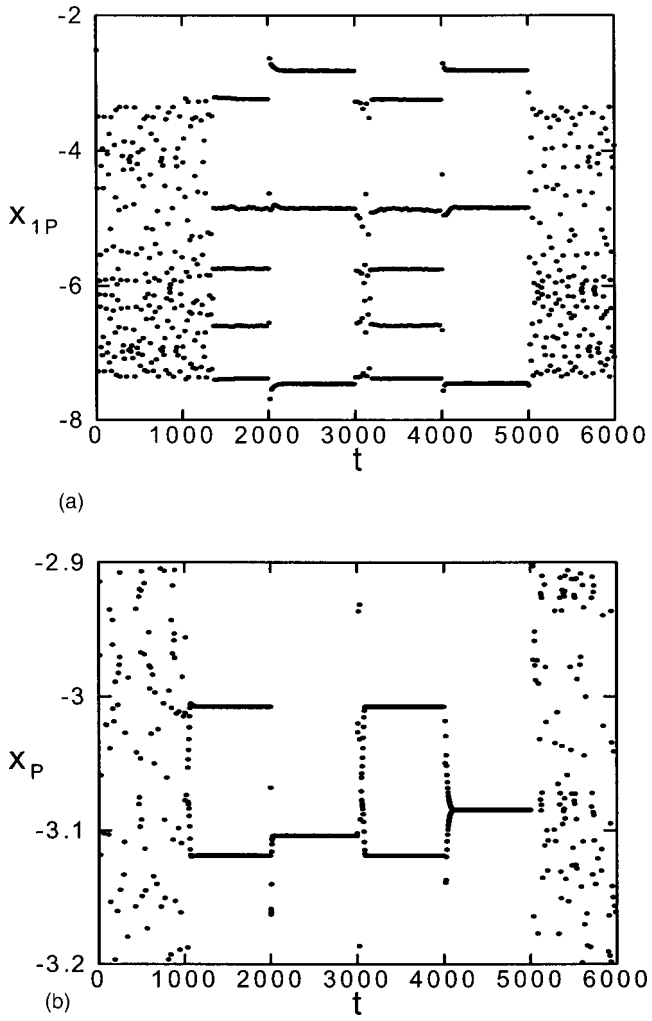

FIG. 9. (a) Switching control of noise-perturbed Rössler system ($\sigma=5\times10^{-4}$) in the time period $t=1000$ to 5000 with alternatively application of the signals $R_{2,2}$ ($P=6.41\times10^{-4}$, P-5) and $R_{2,4}$ ($P=2.08\times10^{-2}$, P-3) every 1000 time units. The phase shifts at various stages are $t=1000:\varphi=2.021\,299\,01; t=2000:\ \varphi=-1.960\,980\,48;\ t=3000:\ \varphi=5.179\,225\,27;\ t=4000:\ \varphi=-3.793784\,08$ and (b) Switching control of noise-perturbed Lorenz system ($\sigma=10^{-4}$). The signal is switched between $L_{2,2}$ ($P=6.20\times10^{-6}$, P-2) and $L_{2,3}$ ($P=1.71\times10^{-5}$, P-1) every 1000 time units. The phase shifts at various stages are $t=1000:\varphi=4.336\,693\,31; t=2000:\ \varphi=-1.890\,718\,84;\ t=3000:\varphi=4.336\,693\,31;\ t=4000:\ \varphi=1.642\,425\,00$.

the state variable x_1 on the Poincaré section $x_2=0$ plotted vs time. Figure 7(b) shows the switching control of the Lorenz system by alternately applying control signals $L_{2,1}$(P-8) and $L_{2,4}$(P-1). The sequence of this process is: CA→P-8→P-1→P-8→P-1→CA. The histogram of x on the Poincaré section $y=-5$ is presented. The transient stage in each switching process is evidently quite short, which is evidence of the control effectiveness of the present chaos control method.

C. Control of noise-perturbed systems

For practical applications of chaos control, the robustness of the method in the presence of noise is significant. The noise can be the external disturbances to the system or the uncertainties due to inexactness in modeling of the system. The Gaussian white noise with zero mean is added to all the state variables of the systems from the initial time instant $t=0$. The noise level is measured by the standard deviation σ of the Gaussian distribution.

To understand the influence of the noise on the controllability, the variation of the largest Lyapunov exponent with the change in the noise level σ is examined. Accurate threshold of the noise level can be determined by measuring the largest Lyapunov exponent. For the control signals $R_{2,1}$ (P-9) and $R_{2,2}$ (P-5), plots of λ_1 vs σ are shown in Figs. 8(a) and 8(b). Each curve presented here represents the average value

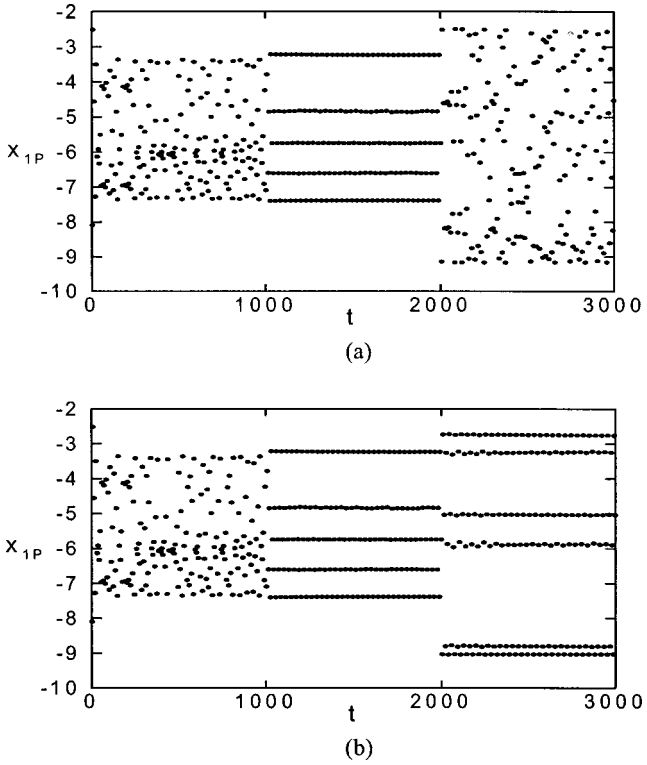

FIG. 10. Control targets of the noise-perturbed Rössler system ($\sigma=5\times10^{-4}$) with abrupt change in the parameter c at $t=2000$. (a) Chaos control by applying $R_{2,3}$ at $t=1000$, parameter c abruptly changes from 4.6 to 5.7 at $t=2000$ but the control signal is unchanged, and (b) the control signal also alters ($P=9.21\times10^{-4}$, P-6) at $t=2000$ for taming the new chaotic behavior.

obtained from ten independent runs with the random number generator reset. One can observe that the stability of the controlled system is destroyed as the noise level σ raised up to a threshold value $\sigma_{\text{th}}\approx2.7\times10^{-7}$ for the signal $R_{2,1}$ and $\sigma_{\text{th}}\approx8.2\times10^{-4}$ for $R_{2,2}$. The results show that the lower the control power is, the less robust the signal. This point was also mentioned in a previous work, Ref. [13]. Similar to the above study for the Rössler system, the stability of the controlled Lorenz system with the influence of noise is shown in Figs. 8(c) and 8(d). The threshold noise level is $\sigma_{\text{th}}\approx1.5\times10^{-2}$ for $L_{2,1}$ and $\sigma_{\text{th}}\approx7.6\times10^{-1}$ for $L_{2,4}$.

The effectiveness of the switching control in the presence of background noise is studied by repeating the cases in Fig. 7. The noise level is set as $\sigma=5\times10^{-4}$ for the Rössler system and $\sigma=10^{-4}$ for the Lorenz system. In Fig. 9(a), the switching signals $R_{2,2}$(P-5) and $R_{2,4}$ (P-3) are employed for the switching sequence of CA$\rightarrow$P-5$\rightarrow$P-3$\rightarrow$P-5$\rightarrow$P-3$\rightarrow$CA. For the Lorenz system, Fig. 9(b) shows the sequence of CA$\rightarrow$P-2$\rightarrow$P-1$\rightarrow$P-2$\rightarrow$P-1$\rightarrow$CA by alternatively applying the control signals $L_{2,2}$ (P-2) and $L_{2,3}$ (P-1). Both cases demonstrate the effectiveness of the present method in noise-disturbed systems. However, comparing with the noise-free counterparts, a little stronger control signals have to be used.

D. Control of noise-disturbed systems with abrupt change in parameters

As an illustrative example, a noise-disturbed Rössler system of chaotic state at $a=b=0.2$ and $c=4.6$ in the presence of a noise level $\sigma=5\times10^{-4}$ is considered. The control input of a two-mode signal is adopted and the perturbation frequency is searched for in the range of $\omega\in[1.0,1.3]$. Figure 10(a) shows that the chaotic behavior of the uncontrolled system is tamed after the control signal $R_{2,3}$ applied at $t=1000$ and the system is led to a periodic motion of period-5. As the parameter c is abruptly changed to the value of $c=5.7$ at $t=2000$, the system behaves chaotically again if the control signal is kept the same. However, by applying a new signal ($P=9.21\times10^{-4}$, P-6) after $t=2000$, the system can be continuously stabilized and brought to a new state of P-6, Fig. 10(b).

IV. CONCLUDING REMARKS

In the present work, we have developed a novel nonfeedback chaos control method with GA-optimized weak periodic perturbation signals. On the two noted nonlinear systems, the Rössler system (external forcing control) and Lorenz system (parametric control), it has been demonstrated that the present method can work effectively and robustly on the systems with and without the presence of a background noise. Besides the above-mentioned merits, the following conclusions can be drawn based on the present results and analysis.

(1) Compared with previous methods, in general, the present approach can achieve the control goal with significantly lower power, ranging from one to three orders of magnitude in difference. The power of each control signal found by this approach does not necessarily decrease with the increase of additional Fourier modes. It has been demonstrated that the present method performs very effectively by using the signal of low modes, i.e., two or three in the cases studied. This fact is especially significant in practical applications, in which the cost of computation is one of the major concerns.

(2) The period number k of the controlled orbit at the final state depends on the power of the control signal. The initial condition does not obviously change the power of the optimized signal and, in turn, no influence on the period number of the orbit. However, using an optimized n-mode signal to construct individuals of $(n+1)$-mode can dramatically shorten the time required for optimization. For the autonomous systems, the phase of the control signal considerably shortens the transient time period before reaching the control target but has little influence on the power of the optimized signal and the period number.

(3) Several topics are worthy of future investigations. For example, besides the periodic control signals of Fourier form, other possibilities, such as step functions, impulse functions, etc., can also be considered. Developing a method to specify the period number of the target state is also an attractive issue. In addition, hybrid algorithms, which use a combination of genetic algorithms and other gradient search techniques to enhance the efficiency of the search, and alternative fitness functions are both interesting and worthwhile for further study.

[1] E. Ott, C. Grebogi, and J. A. Yorke, Phys. Rev. Lett. **64**, 1196 (1990).
[2] J. Singer, Y. Z. Wang, and H. H. Bau, Phys. Rev. Lett. **66**, 1123 (1991).
[3] K. Pyragas, Phys. Lett. A **170**, 421 (1992).
[4] K. Yagasaki and T. Uozumi, Phys. Lett. A **238**, 349 (1998).
[5] C. C. Hwang, R. F. Fung, J. Y. Hsieh, and W. J. Li, Int. J. Eng. Sci. **37**, 1893 (1999).
[6] G. Chen and X. Yu, IEEE Trans. Circuits Syst., I: Fundam. Theory Appl. **46**, 767 (1999).
[7] R. Lima and M. Pettini, Phys. Rev. A **41**, 726 (1990).
[8] Y. Braiman and I. Goldhirsch, Phys. Rev. Lett. **66**, 2545 (1991).
[9] L. Fronzoni, M. Giocondo, and M. Pettini, Phys. Rev. A **43**, 6483 (1991).
[10] Y. Lui and J. R. Leite, Phys. Lett. A **185**, 35 (1994).
[11] M. Kraus, J. Müller, D. Lebender, and F. W. Schneider, Chem. Phys. Lett. **260**, 51 (1996).
[12] A. Guderian, A. F. Münster, M. Jinguji, M. Kraus, and F. W. Schneider, Chem. Phys. Lett. **312**, 440 (1999).
[13] R. Mettin and T. Kurz, Phys. Lett. A **206**, 331 (1995).
[14] K. Murali, M. Lakshmanan, and L. O. Chua, Int. J. Bifurcation Chaos Appl. Sci. Eng. **5**, 563 (1995).
[15] E. A. Jackson, Phys. Rev. A **44**, 4839 (1991).
[16] S. Rajasekar, Phys. Rev. E **51**, 775 (1995).
[17] S. Rajasekar, K. Murali, and M. Lakshmanan, Chaos, Solitons Fractals **8**, 1545 (1997).
[18] M. Ramesh and S. Narayanan, Chaos, Solitons Fractals **10**, 1473 (1999).
[19] D. E. Goldberg, *Genetic Algorithms in Search, Optimization, and Machine Learning* (Addison-Wesley, New York, 1989).
[20] Z. Michalewicz, *Genetic* Algorithms+Data Structures= *Evolution Programs* (Springer, New York, 1992).
[21] O. E. Rössler, Phys. Lett. **57A**, 397 (1976).
[22] E. N. Lorenz, J. Atmos. Sci. **20**, 130 (1963).
[23] J. Yang, Z. Qu, and G. Hu, Phys. Rev. E **53**, 4402 (1996).
[24] A. Wolf, J. B. Swift, H. L. Swinney, and J. A. Vastano, Physica D **16**, 285 (1985).
[25] M. Sano and Y. Sawada, Phys. Rev. Lett. **55**, 1082 (1985).
[26] J.-P. Eckmann, S. O. Kamphorst, D. Ruelle, and S. Ciliberto, Phys. Rev. A **34**, 4971 (1986).
[27] X. Zeng, R. Eykholt, and R. A. Pielke, Phys. Rev. Lett. **66**, 3229 (1991).
[28] J. B. Gao, Phys. Rev. E **63**, 066202 (2001).